SYNTHESIS OF BENTONITE/ALGINATE COMPOSITE BEADS AND THEIR APPLICATION FOR ADSORPTION OF CRYSTAL VIOLET DYE

Thieu Quang Quoc Viet, Tran Nguyen Phuong Lan, Ly Kim Phung*

Can Tho University

ARTICLE INFO **ABSTRACT**

Received: 28/6/2025 Revised:

21/11/2025

Published: 25/11/2025

KEYWORDS

Activated bentonite/ alginate composite bead Natural mineral Adsorption Crystal violet Efficient reuse

This study synthesized the composite beads based on bentonite sources in Vietnam and alginate for the adsorption of crystal violet in wastewater. The characteristic properties of bentonite and alginate in the beads were determined by Fourier-transform infrared spectroscopy, X-ray diffraction, thermogravimetric analysis, and scanning electron microscopy methods. The functional groups of both bentonite and alginate could be found in the composite. At the same time, the morphology of the composite beads were spherical beads with a rough surface. The crystal violet removal under different conditions, including adsorbent dosage, initial crystal violet concentration, contact time, and competitive ions, was investigated. The adsorption efficiency was 90.45% under pH 7, an adsorbent dosage of 1 g/L, and an initial crystal violet concentration of 138.82 mg/L within 90 min. Especially, the adsorption efficiency value was maintained above 70% in the environment containing competing ions such as Na⁺, K⁺, Ca²⁺, Mg²⁺, and their mixture. The experimental data were in good agreement with the Sips model ($R^2 = 0.989$) and the pseudo-first-order kinetic model ($R^2 = 0.999$). After 10 cycles, the adsorption efficiency reduced by about 12.29% compared to the first round. These findings suggest that the synthesized composite beads can be a promising absorbent for the dye removal in wastewater.

TỔNG HỌP HẠT COMPOSITE BENTONITE/ALGINATE VÀ ÚNG DỤNG HÁP PHU THUỐC NHUÔM CRYSTAL VIOLET

Thiều Quang Quốc Việt, Trần Nguyễn Phương Lan, Lý Kim Phụng* Đại học Cần Thơ

THÔNG TIN BÀI BÁO

TÓM TẮT

Ngày nhận bài: 28/6/2025 Ngày hoàn thiện: 21/11/2025

Ngày đăng: 25/11/2025

TỪ KHÓA

Hat composite activated bentonite/ alginate Khoáng tư nhiên Hấp phụ Crystal violet Tái sử dụng hiệu quả

Nghiên cứu đã tổng hợp hạt composite dựa trên nguồn bentonite tại Việt Nam và alginate hướng đến ứng dụng hấp phụ thuốc nhuộm crystal violet. Các đặc tính của bentonite và alginate được xác định bởi phương pháp phổ hồng ngoại biến đổi Fourier, nhiễu xạ tia X, phân tích nhiệt trọng lượng và kính hiển vi điện tử quét. Các nhóm chức của bentonite và alginate có thể được tìm thấy trong composite. Đồng thời, hình thái của các hạt composite là các hạt cầu với bề mặt gồ ghề. Khả năng hấp phụ crystal violet tại các điều kiện khác nhau bao gồm liều lượng chất hấp phụ, nồng độ ban đầu của crystal violet, thời gian và các ion canh tranh đã được khảo sát. Hiệu suất là 90,45% tại pH 7, liều lượng chất hấp phụ là 1 g/L, nồng độ ban đầu của crystal violet là 138,82 mg/L trong 90 phút. Đặc biệt, hiệu suất vẫn được duy trì trên 70% trong môi trường tồn tại các ion cạnh tranh như Na⁺, K⁺, Ca²⁺, Mg²⁺ và hỗn hợp ions. Dữ liệu thực nghiệm phù hợp tốt với mô hình Sips $(R^2 = 0.989)$ và mô hình động học giả định bậc $1 (R^2 = 0.999)$. Sau 10 chu kỳ, hiệu suất giảm khoảng 12,29% so với lần hấp phụ đầu tiên. Những phát hiện này cho thấy hạt composite có thể là chất hấp phụ đầy hứa hẹn để loại bỏ thuốc nhuộm trong nước thải.

DOI: https://doi.org/10.34238/tnu-jst.13144

300 Email: jst@tnu.edu.vn http://jst.tnu.edu.vn

Corresponding author. Email: lkphung@ctu.edu.vn

1. Introduction

Although rapid industrialization and population growth have driven global economic progress, they pose serious environmental risks, especially water pollution [1]. Wastewaters containing hazardous substances such as heavy metals and organic dyes present significant threats to public health and ecosystems [2], [3]. Crystal violet (CV), a common cationic dye used in textile industries and laboratories, is highly persistent, bioaccumulative, and toxic [2]. Various methods, namely advanced oxidation, membrane filtration, and adsorption, have been investigated to remove CV [4]. Among them, the adsorption offers distinct advantages, including low cost and process simplicity [2], [3]. A key challenge also lies in selecting effective adsorbents for dye removal. Research on natural materials like bentonite, alginate (Alg), chitosan, and carrageenan has been conducted by many researchers [5] - [7]. Natural clays have attracted considerable interest as adsorbents due to their abundance, low cost, and eco-friendly properties [1]. Bentonite, one of the most prevalent clay minerals, features a layered structure with octahedral aluminum sheets sandwiched between tetrahedral silicon sheets [2]. Ionic substitutions within these layers impart a net negative surface charge, yielding high AC and strong ion exchange properties [2], [8]. However, the fine particle size of bentonite complicates its separation from aqueous solutions after use, increasing further processing steps and overall treatment costs [3]. To overcome this limitation, bentonite is commonly incorporated into composites to enlarge its particle size, simplify recovery, and enhance the dye removal performance. Alg is a natural polymer derived from brown algae with a structure consisting of β-D-mannuronic acid and α-L-guluronic acid units as copolymers [1]. Due to its biocompatibility and gel-forming capacity, Alg has been widely employed in various applications, including the adsorption of environmental pollutants such as pharmaceuticals and biologically active substances [1]. The combination of bentonite from Vietnam and Alg to generate the composite beads was performed in this study. Several methods, such as Fourier-transform infrared spectroscopy (FTIR), X-ray diffraction (XRD), thermogravimetric analysis (TGA), and scanning electron microscopy (SEM), were used to characterize materials. The AC of CV using the composite beads was evaluated at different operating conditions such as adsorbent dosage (0.5 - 2.0 g/L), initial CV concentration (24.47 -211.76 mg/L), and contact time (15 - 1440 min). Besides, the mechanisms of the adsorption process can be explored through fitting adsorption isotherms and kinetics models. The regeneration ability of the beads after CV adsorption was also carried out.

2. Materials and Methods

2.1. Materials and chemicals

Raw bentonite (RB) was obtained from Lam Dong province, Vietnam, whereas Alg was derived from brown algae, produced in China. Other chemicals such as calcium chloride (CaCl₂, 99%), sodium hydroxide (NaOH, 96%), hydrochloric acid (HCl, 36.5%), potassium chloride (KCl, 99%), crystal violet ($C_{25}H_{30}N_3Cl$, 99%), and ethanol (C_2H_5OH , 99.7%) were supplied from Xilong, China.

2.2. Synthesis of AB/Alg composite beads

The acid activation process was carried out by placing raw bentonite and 0.5 M HCl solution in a two-necked flask at a solid and liquid ratio of 5:1 (w/v) [3]. The suspension was stirred at a speed of 300 rpm, 40°C for 1 h. Then, the mixture was washed to neutral pH and dried until constant weight to obtain the acid-activated bentonite (AB). The fabrication of beads was based on previous studies with some modifications [1], [3]. Gel of Alg was prepared by dissolving Alg powder in 50 mL of distilled water at room temperature. Then, a precise amount of AB was added to the Alg gel and stirred at room temperature to form a suspension. Next, an AB/Alg precursor mixture was obtained by slowly adding AB to Alg gel and was thoroughly stirred for

30 min. After that, the mixture was slowly added into the CaCl₂ solution to form the beads using a syringe with a tip size of 0.2 mm. After being immersed in the solution for a certain time to create the cross-linking with Alg molecules, AB/Alg composite beads were collected and washed to neutral pH. The synthesized beads were dried using a freeze dryer (Laboncon, USA) at -50 °C and 0.5 mbar for 24 h.

2.3. Characterization of AB/Alg beads

Properties of AB, Alg, and beads were examined using some advance methods such as FTIR, XRD, and TGA. The characteristic vibrations of bonding existing in beads were determined by FTIR (Jasco FT/IR 4600, Japan). Thermal stability analysis of the composite was applied using LABSYS evo (Setaram, France) under N_2 gas flow with a heating rate of 10 °C/min in the range from room temperature to 800 °C. The D8 diffractometer (Bruker, Germany) was operated at the 20 angle scanning range from 20 to 80° at room temperature with CuK α radiation (λ = 1.5406 Å) to obtain the characteristic diffraction peaks of beads. Moreover, the morphology of beads was observed through SEM images (S4800, Hitachi, Japan). The isoelectric point of beads was also determined by impregnation with KCl [2].

2.4. Adsorption experiments

The CV adsorption of beads was conducted by varying operating conditions such as adsorbent dosage (0.5-2.0 g/L), initial CV concentration (24.47 - 211.76 mg/L), contact time (15-1440 min), and the presence of competitive ions $(Na^+, K^+, Ca^{2+}, Mg^{2+}, \text{ and their mixture})$ at a concentration of 0.01 M. The adsorption process was performed by adding 0.05 g of beads into 50 mL of 100 mg/L CV solution, shaking for 60 min at room temperature. The liquid fraction was then collected, and the CV concentration was analyzed after adsorption. Both initial and final CV concentrations $(C_o \text{ and } C_t)$ were determined by a UV-vis spectrometer (Multiskan SkyHigh, Thermo Fisher Scientific, USA) at $\lambda_{max} = 590 \text{ nm}$ [6]. The other conditions were similarly experimented as previously described. The AE and AC were calculated based on formulas (1) and (2).

and AC were calculated based on formulas (1) and (2).

$$AE (\%) = \frac{(C_0 - C_t) \times V}{m}$$
(1)
$$AC \left(\frac{mg}{g}\right) = \frac{C_0 - C_t}{C_0} \times 100$$
(2)

where m (g) and V (L) are the mass of beads and volume of CV solution used, respectively. Adsorption isotherm (Langmuir, Freundlich, and Sips) and adsorption kinetic (pseudo-first-order (PFO), pseudo-second-order (PSO), and intraparticle diffusion) models were applied to explore the mechanisms of CV adsorption using AB/Alg composite beads in this work.

2.5. Regeneration of AB/Alg composite beads

After freeze-drying (-50 °C and 0.5 mbar) for 24 h, beads were desorbed in ethanol (a solid: liquid ratio = 2:1 g/L) at 200 rpm for 90 min [9]. The reused beads were then rinsed, freeze-dried, and used for subsequent cycles. The AE of reused beads was calculated based on formula (1).

3. Results and discussion

3.1. Properties of AB/Alg composite beads

The characteristic vibrations of AB, Alg, and the beads are shown in Figure 1a. The FTIR spectrum of AB including the vibration at 3615.88 cm⁻¹ corresponds to the –OH stretching vibrations of adsorbed water on the material surface [8], [10] while the peaks at 1644.02 and 1001.84 cm⁻¹ reflect the –OH bending and Si–O–Si [8]. Bands of 500 – 900 cm⁻¹ indicate Al–Al–OH, Al–O, Al–OH, and Si–O–Al vibrations in tetrahedral and octahedral sheets [8]. In the Alg spectrum, the vibration at 3244.65 cm⁻¹ represents the hydroxyl groups in the mannuronic acid and uronic acid units of Alg [11]. Besides, the characteristic bands of Alg are determined at 1594.84 and 1408.75 cm⁻¹, which are assigned to the asymmetric stretching and symmetric stretching of the -COO group, respectively [10]. The mannuronic acid and uronic acid groups of

Alg are identified at the range of 700 – 900 cm⁻¹ [11]. In the FTIR spectrum of beads, the shift of the vibration representing the hydroxyl group to the wavenumber of 3364.21 cm⁻¹ can be explained by the hydrogen bonding between AB and Alg during the composite formation [7]. The Si-OH bond of AB appears at the band of 1630.52 cm⁻¹ [11], [12], meanwhile, several characteristic vibrations are overlapped and shifted; the asymmetric and symmetric –COO stretches occur at 1531.78 and 1422.24 cm⁻¹ due to chelation between hydroxyl/carboxyl groups and Ca²⁺ [11]. The band of Si-O-Si shifted to 1019.19 cm⁻¹ in the beads owing to Alg-AB interactions. The tetrahedral and octahedral structures of AB are not fully revealed because of the shielding of Alg molecules. However, the vibrations at 916.02 and 688.79 cm⁻¹ are characteristic vibrations for the Al-Al-OH and Si-O groups of AB, respectively. The FTIR spectra indicated that AB is effectively embedded within the Alg matrix with supporting by the cross-linking agent.

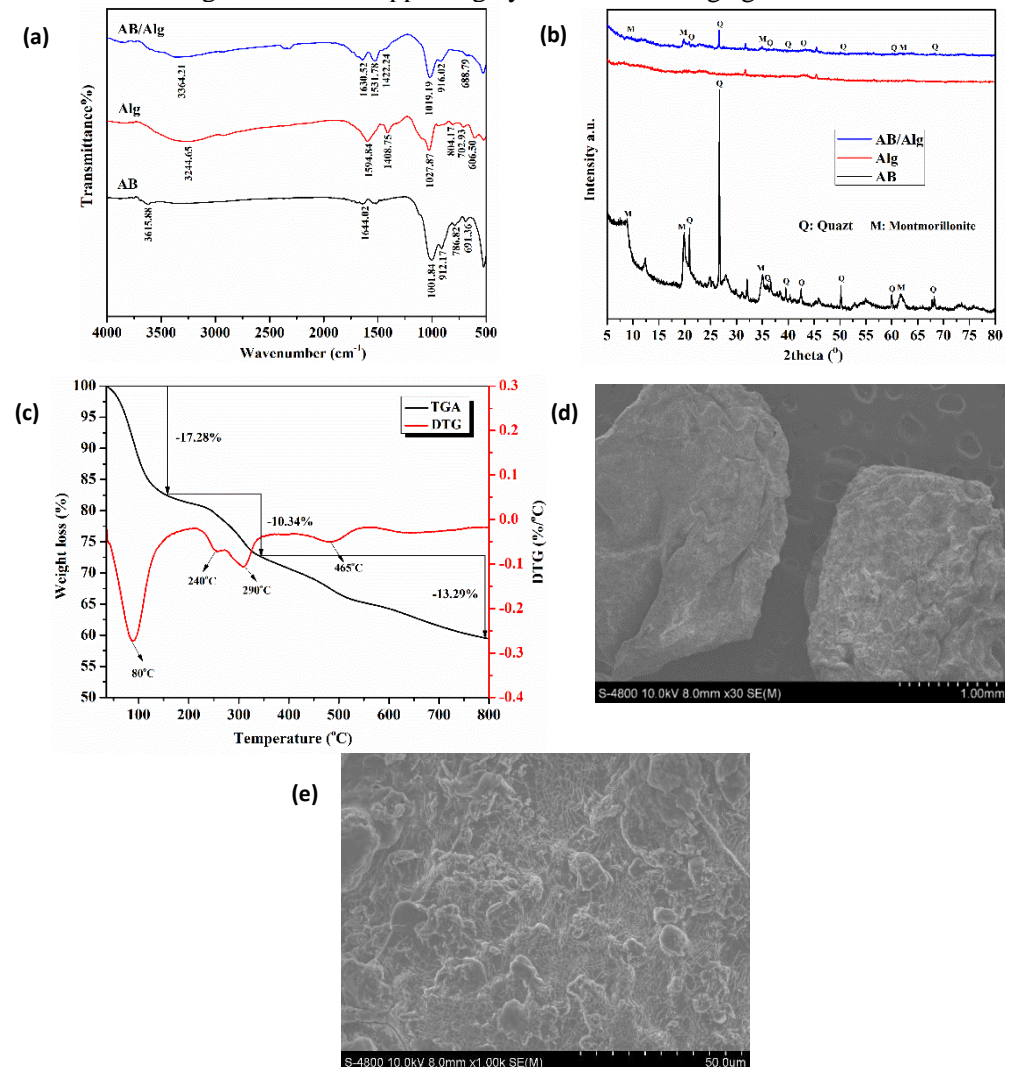


Figure 1. FTIR spectra (a), XRD pattern (b), TGA-DTG results (c), and SEM images of AB/Alg beads at different magnification (d-e)

The XRD patterns of AB, Alg and AB/Alg beads are found in Figure 1b. AB exhibits characteristic montmorillonite peaks at $2\theta = 8.48^{\circ}$, 20.90° , 35.03° , and 61.74° [4], while quartz peaks appear at $2\theta = 21.37^{\circ}$, 26.70° , 36.60° , 39.52° , 42.49° , 51.02° , 60.03° , and 67.17° [13]. Besides, Alg and beads are mostly amorphous due to the intrinsic amorphous nature of Alg [4]. However, peaks at 8.61° , 20.82° , 34.95° , 61.68° (montmorillonite) and 21.61° , 26.63° , 36.68° ,

39.28°, 42.43°, 51.05°, 60.13°, 68.30° (quartz) in AB/Alg indicate the maintenance of these phases. The minimal shift suggested that its structure is preserved during composite bead formation [4].

Thermogravimetric analysis of AB/Alg beads is found in Figure 1c. Below 150 °C, the mass loss of the beads is about 17.28% and reaches 23.63% in the range of 150 – 800 °C. From the DTG curves, the maximum mass loss peaks of the beads can be suggested in three main steps of the thermal degradation process: First, the evaporation of water molecules results in a dehydrated state of samples at below 150 °C [14]. The second step is the degradation of glycosidic bonds at 150 – 250 °C, which initiates a significant structural deterioration of the beads [3]. The mass loss at temperatures above 250 °C is attributed to two main reasons, including (i) the release of hydroxyl groups within the AB structure and (ii) the decomposition of intermediate organic compounds to form inorganic and char residues [3]. This is demonstrated through three peaks at 240 °C, 295 °C and 465 °C, respectively. The surface morphologies of AB/Alg beads (Figure 1d) reveal a predominantly spherical shape with a rough surface texture, and bead sizes are lower than 1mm. These morphological features are attributed to the cross-linked Alg-Ca²⁺ matrix [4], [7]. Similar surface characteristics have been reported in previous studies, including bentonite/Alg beads [4] and whey/Alg composite beads [7].

3.2. The CV removal using AB/Alg composite beads

The isoelectric point of beads is 6.37, meaning that at pH < 6.37, the bead surface is covered with a layer of positive charge and vice versa. Therefore, the CV adsorption of AB/Alg is comprehensively evaluated in a neutral pH environment. The effect of bead dosage on AC and AE using AB/Alg is performed at pH 7, an initial CV concentration of 103.53 mg/L during 60 min (Figure 2a). An increase of the dosage from 0.5 to 2.0 g/L enhanced the AE from 50.19 to 91.72%, which was similarly found in previous studies [12], [15]. More material dosage used resulted in more adsorption sites added in the system, facilitating the capture of CV molecules [2], [15]. In contrast, ACs dramatically decrease between 102.75 and 46.94 mg/g with an increase in a dosage of 0.5 - 2.0 g/L due to the overloading of active sites, causing waste of adsorbent [12], [15]. In this study, an adsorbent dosage of 1.0 g/L is chosen to ensure high AE and limit the waste of AB/Alg.

The effect of initial CV concentrations from 24.47 to 211.76 mg/L on AE and AC of beads is examined at pH 7, an adsorbent dosage of 1 g/L within 60 min (Figure 2b). The AE reaches a maximum value of 97.44% at 24.47 mg/L, then decreases with higher concentrations of CV loaded, and drops to the lowest value of 62.41% at 211.76 mg/L. The high AEs achieved at low CV concentrations were due to the lower ratio of dye molecules to available adsorption sites [2], [12]. At the higher CV concentrations, the adsorption sites become saturated, leading to the AE reduction. Meanwhile, ACs rapidly increase from 23.84 to 132.16 mg/g as the initial concentrations are increased between 24.47 and 211.76 mg/L. The substantial increase in AC with rising CV concentration is mainly due to the greater surface coverage of beads by CV molecules [15] and enhancement of the mass transfer kinetics at the higher CV concentration [16]. With the high AE and AC of 82.87% and 113.10 mg/g, respectively, the initial CV concentration of 138.82 mg/L is selected for subsequent experiments.

Figure 2c exhibits the effect of various contact time from 15 to 1440 min on the CV adsorption performance using AB/Alg at the fixed condition of pH 7, an adsorbent dosage of 1 g/L, and an initial concentration of 138.82 mg/L. At the early stage (15 – 45 min), both AEs and ACs significantly increase from 41.38 to 62.22% and 57.45 to 91.71 mg/g, respectively. Doubling the contact time to 90 min, the AE and AC reach 90.45% and 125.57 mg/g, respectively. The adsorption ability of beads slightly enhances and remains constant after 720 min. A stepwise variation of AE and AC values during the initial adsorption period (15 – 90 min) was also observed, which describes the high availability of adsorption sites [7]. The saturation of active sites led to a negligible change in AE and AC at the prolonged adsorption time [6]. In this

work, AE and AC are 90.45% and 125.57 mg/g after 90 min, respectively, indicating the fast adsorption ability of AB/Alg.

The effect of competing ions on the CV adsorption of beads is investigated, as shown in Figure 2d, under the optimal operating conditions. In the presence of Na⁺ and K⁺, the AE and AC seem to be slightly changed compared to those without ions added. Meanwhile, Ca²⁺ and Mg²⁺ ions significantly affected the AE and AC of beads, especially Ca²⁺ ions. The AE and AC drop to the lowest values (76.29% and 103.22 mg/g) in the presence of Ca²⁺ ions and slightly decrease in the presence of Mg²⁺ ions due to the charge differences between monovalent ions and divalent ions [17]. The less pronounced decrease in AE and AC in the presence of Mg²⁺ ions may be attributed to their higher hydration compared to Ca²⁺, which limits their ability to interact with the functional groups of Alg and AB [1]. Additionally, more cations loaded will densify the bead network, causing a significant reduction of AE and AC. Cations also weaken the electrostatic interactions between the bead adsorption sites and CV [19]. This led to the lower AE and AC observed in the media with the addition of competing ions. Despite the decrease, the AE of CV adsorption remains higher than 70%, revealing their potential in the treatment of dye-containing wastewater.

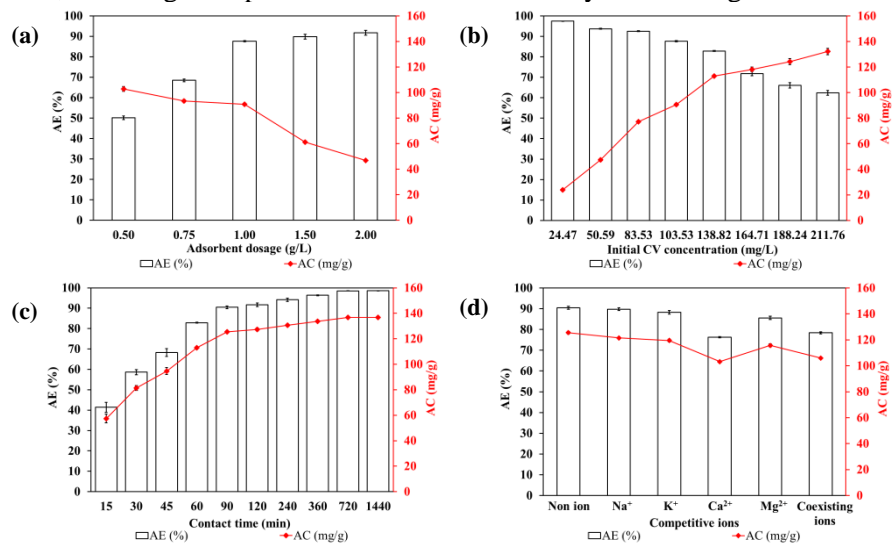


Figure 2. The CV removal ability using beads at different operating conditions: adsorbent dosage (a), initial CV concentration (b), contact time (c), and competitive ions (d)

3.3. Isotherm and kinetic models

The interaction mechanisms between beads and CV molecules are explored through fitting the experimental data with isotherms such as Langmuir, Freundlich, and Sips (Table 1). The Sips model with $R^2=0.989$ best describes the CV adsorption mechanism of beads. With the $n_{\rm S}$ coefficient of 0.7833, the monolayer adsorption mechanism seems to be more dominant in the CV adsorption. The maximum adsorption capacities from the Langmuir and Sips models are 145.67 and 147.65 mg/g, respectively, suggesting favorable interactions between AB/Alg and CV, and the energy is uniform among the adsorption sites [1]. Besides, the actual adsorption process includes both homogeneous and heterogeneous adsorption of the Sips model. Based on parameters of the isotherm models, the mechanism of the CV adsorption process can be proposed to include both single-layer and multilayer adsorption.

In Table 1, the equilibrium AC values calculated from PFO (133.446 mg/g) and PSO (142.94 mg/g) models also express a good agreement with the experimental equilibrium AC value at 24 h (136.85 mg/g). Corresponding to the R^2 value, it can be seen that the AC from PFO has a closer value to the experimental AC than the AC from PSO. This indicated that the experimental

http://jst.tnu.edu.vn 305 Email: jst@tnu.edu.vn

adsorption fits the PFO model better ($R^2 = 0.999$) and the CV adsorption rate of the beads depended on the available sites on the material and the dye concentration [1]. At the same time, the physical adsorption happened between many pores of the beads and CV, positively contributing to the adsorption mechanism [1], [4]. The adsorption process involved CV transfer from the solution to the solid phase via intraparticle diffusion, which is often the rate-limiting step in adsorption processes [1]. With a R^2 of 0.968, the intraparticle diffusion is not the only rate-limiting step in adsorption. From the above observations, the adsorption rate is mainly controlled by the interactions between the available active sites on the beads and CV.

Table 1. Parameters of adsorption isotherm and kinetic models

Adsorption i	sotherm models		
Model	Equation	Parameter	Value
		Q_t (mg/g): the AC at time t	-
Langmuir	$Q_{t} = \frac{Q_{\text{max}} K_{L} C_{e}}{1 + K_{L} C_{e}} $ (3)	Q_{max} (mg/g): the Langmuir maximum AC K_L (L/mg): the Langmuir adsorption equilibrium constant	145.670
		K _L (L/mg): the Langmuir adsorption equilibrium constant	0.198
		R^2	0.955
	1	K_F ((mg/g)(mg/L): the Freundlich isotherm constant	42.108
Freudlich	$Q_{t} = K_{F} C_{e}^{\frac{1}{n_{F}}} (4)$	n _F : the constant related to the heterogeneity of the adsorbent	3.651
		R^2	0.936
		Q_S (mg/g): the Sips maximum AC	147.650
Sips	$Q_{t} = \frac{Q_{S}\alpha_{S}C_{e}^{n_{S}}}{1 + \alpha_{S}C_{e}^{n_{S}}} (5)$	$\alpha_{\rm S}$ (L/mg): the Sips equilibrium constant	0.232
		n _s : the Sips model exponent	0.783
		R^2	0.989
Adsorption l	kinetic models		
Model	Equation	Parameter	Value
		t (min): time	-
PFO	Q_t = $Q_e (1 - e^{-k_1 t}) (6)$	Q _e (mg/g): the equilibrium AC	133.446
		k ₁ (1/min): the PFO rate constant	0.031
		R^2	0.999
	1 02	$O_{s}(m\sigma/\sigma)$	142.940

$\begin{array}{c} \text{PFO} & = Q_{e} \left(1 - e^{-k_{1}t} \right) \text{ (6)} & k_{1} \left(1/\text{min} \right) \text{: the PFO rate constant} \\ R^{2} & 0.999 \\ \text{PSO} & Q_{t} = \frac{k_{2}Q_{e}^{2}t}{1 + k_{2}Q_{e}t_{e}} \text{ (7)} & k_{2} \left(g/\text{mg.min} \right) \text{: the PSO rate constant} \\ R^{2} & 0.999 \\ k_{2} \left(g/\text{mg.min} \right) \text{: the PSO rate constant} \\ R^{2} & 0.998 \\ \\ \text{Intraparticle diffusion} & Q_{t} = k_{i}(t)^{0.5} + C_{i} \text{ (8)} & C_{i} \left(\text{mg/g.min} \right) \text{: the intraparticle diffusion rate constant} \\ R^{2} & 0.968 \\ \end{array}$

3.4. The potential reuse of beads

The reusability of beads is performed at the optimal adsorption conditions as indicated in Figure 3a. The AE slightly decreased and reached 78.16% after the 10th adsorption cycle. The FTIR spectra of the fresh beads, the adsorbed beads, and the desorbed beads show that the characteristic vibrations of AB and Alg are almost completely maintained after one adsorptiondesorption cycle, indicating the stability of the beads. However, slight shifts and broadening of these bands occur compared to the original composite, especially in the $500 - 2000 \text{ cm}^{-1}$ range. In the adsorbed beads, vibrations at 1368.25 cm⁻¹ and 1165.76 cm⁻¹, representing the stretching vibrations of the -C-N group (CV dye) [7]. The absence of 1100 cm⁻¹ after desorption proves the successful desorption of CV molecules using the beads. Based on the above findings, the proposed CV adsorption mechanism of the composites is primarily governed by electrostatic interactions between the negatively charged surface of the composite and CV⁺ ions, supported by an additional pore-filling mechanism. Composites derived from biopolymers, including chitosan, cellulose, carrageenan, and Alg, exhibited high ACs for CV dyes, as shown in Table 2 [5] - [7], [20]. With a mild adsorption condition at pH 5 - 8 and a relatively low dosage of adsorbent required (0.4 - 1.5 g/L), these composites provided an accessible and low-cost adsorption process. Powdered adsorbents required only 20 – 30 min contact time [5], [20], while bead-based adsorbent needed a longer time to allow CV to diffuse into the adsorption sites [6], [7]. In this

study, AB/Alg beads reach the Langmuir maximum AC of 145.67 mg/g, respectively, confirming their strong CV removal and potential as efficient adsorbents.

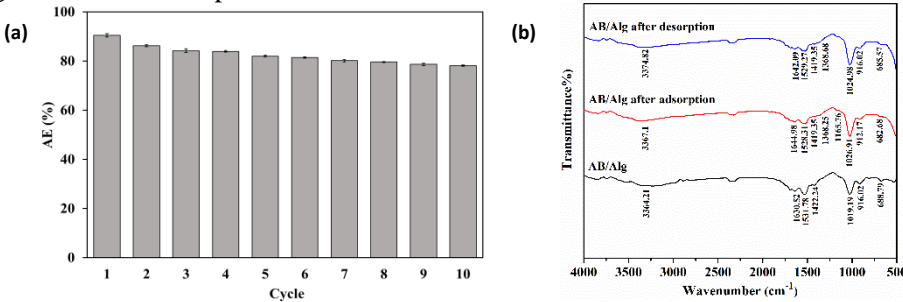


Figure 3. Reuse cycles of beads (a), and FTIR spectra of the fresh beads, the adsorbed beads, and the desorbed beads (b)

Table 2. CV removal capacity of several different materials

Type of adsorbent	Adsorption conditions	$^*Q_{max}$ (mg/g)	Ref.
Bentonite/chitosan	pH 5.0, adsorbent dosage of 1.5 g/L, $**[CV] = 50$ mg/L in 20 min	117.00	[5]
Cellulose-based sugarcane bagasse	pH 7.0, adsorbent dosage of 1.0 g/L, $**[CV] = 40 \text{ mg/L}$ in 30 min	107.50	[20]
Carrageenan/Alg/ montmorillonite	pH 6.8, adsorbent dosage of 1.0 g/L, ** [CV] = 100 mg/L in 250 min	85.20	[6]
Whey/Alg	pH 6.0, adsorbent dosage of 0.4 g/L, ***[CV] = 100 mg/L in 120 h	220.00	[7]
AB/Alg beads	pH 7.0, adsorbent dosage of 1.0 g/L, ** [CV] = 125 mg/L in 90 min	145.67	This study

Q_{max}: the Langmuir maximum AC; **[CV]: the initial CV concentration

4. Conclusion

The AB/Alg composite beads were successfully fabricated in this study using bentonite originating from Vietnam. The physical and chemical properties of the beads were determined through FTIR, XRD, TGA, and SEM. The FTIR spectra showed the characteristic groups of Alg and AB while the organic and inorganic components of beads were also demonstrated through TGA-DTG. The composite beads exhibited a high CV removal under various operating conditions, with the maximum AE of 90.45%. The adsorption process was well fitted to the Langmuir model, and the PFO model with the maximum AC of 145.67 mg/g according to the Langmuir. The adsorption mechanism includes both single-layer and multilayer, driven by electrostatic interactions between the negatively charged surface and cationic dye molecules. Notably, the beads displayed excellent reusability, retaining 78.16% removal efficiency after ten regeneration cycles.

Acknowledgements

This study is funded by Can Tho University, Code: T2024-82.

REFERENCES

- [1] N. Belhouchat, H. Zaghouane-Boudiaf, and C. Viseras, "Removal of anionic and cationic dyes from aqueous solution with activated organo-bentonite/sodium alginate encapsulated beads," *Applied Clay Science*, vol. 135, pp. 9-15, 2017.
- [2] A. A. Oladipo and M. Gazi, "Enhanced removal of crystal violet by low cost alginate/acid activated bentonite composite beads: optimization and modelling using non-linear regression technique," *Journal of Water Process Engineering*, vol. 2, pp. 43-52, 2014.
- [3] R. R. Pawar, Lalhmunsiama, G. I. Pravin, *et al.*, "Use of activated bentonite-alginate composite beads for efficient removal of toxic Cu²⁺ and Pb²⁺ ions from aquatic environment," *International Journal of Biological Macromolecules*, vol. 164, pp. 3145-3154, 2020.

http://jst.tnu.edu.vn 307 Email: jst@tnu.edu.vn

- [4] R. Fabryanty, C. Valencia, F. E. Soetaredjo, et al., "Removal of crystal violet dye by adsorption using bentonite-alginate composite," *Journal of Environmental Chemical Engineering*, vol. 5, pp. 5677-5687, 2017.
- [5] S. E. Elashery, M. M. El-Bouraie, E. A. Abdelgawad, et al., "Adsorptive performance of bentonite-chitosan nanocomposite as a dual antibacterial and reusable adsorbent for Reactive Red 195 and crystal violet removal: kinetic and thermodynamic studies," *Biomass Conversion and Biorefinery*, vol. 15, pp. 2511-2524, 2025.
- [6] G. R. Mahdavinia, H. Aghaie, H. Sheykhloie, et al., "Synthesis of CarAlg/MMt nanocomposite hydrogels and adsorption of cationic crystal violet," *Carbohydrate Polymers*, vol. 98, pp. 358-365, 2013.
- [7] A. Djelad, A. Mokhtar, A. Khelifa, *et al.*, "Alginate-whey an effective and green adsorbent for crystal violet removal: Kinetic, thermodynamic and mechanism studies," *International Journal of Biological Macromolecules*, vol. 139, pp. 944-954, 2019.
- [8] Y. S. Chang, P. I. Au, N. M. Mubarak, *et al.*, "Adsorption of Cu (II) and Ni (II) ions from wastewater onto bentonite and bentonite/GO composite," *Environmental Science and Pollution Research*, vol. 27, pp. 33270-33296, 2020.
- [9] X. Xing, H. Qu, R. Shao, *et al.*, "Mechanism and kinetics of dye desorption from dye-loaded carbon (XC-72) with alcohol-water system as desorbent," *Water Science and Technology*, vol. 76, pp. 1243-1250, 2017.
- [10] R. Pereira, A. Tojeira, D. C. Vaz, et al., "Preparation and characterization of films based on alginate and aloe vera," *International Journal of Polymer Analysis and Characterization*, vol. 16, pp. 449-464, 2011
- [11] H. Daemi and M. Barikani, "Synthesis and characterization of calcium alginate nanoparticles, sodium homopolymannuronate salt and its calcium nanoparticles," *Scientia Iranica*, vol. 19, pp. 2023-2028, 2012.
- [12] K. Akin, V. Ugraskan, B. Isik, et al., "Adsorptive removal of crystal violet from wastewater using sodium alginate-gelatin-montmorillonite ternary composite microbeads," *International Journal of Biological Macromolecules*, vol. 223, pp. 543-554, 2022.
- [13] M. R. Abukhadra, S. M. Ibrahim, S. M. Yakout, *et al.*, "Synthesis of Na⁺ trapped bentonite/zeolite-P composite as a novel catalyst for effective production of biodiesel from palm oil; Effect of ultrasonic irradiation and mechanism," *Energy Conversion and Management*, vol. 196, pp. 739-750, 2019.
- [14] R. Et-tanteny, B. El Amrani, and M. Benhamou, "Investigation and modeling of physicochemical properties of bentonite-chitosan composites versus the concentration of chitosan added by intercalation," *Chemical Physics Impact*, vol. 8, 2024, Art. no. 100611.
- [15] A. Nasrullah, A. Bhat, A. Naeem, *et al.*, "High surface area mesoporous activated carbon-alginate beads for efficient removal of methylene blue," *International Journal of Biological Macromolecules*, vol. 107, pp. 1792-1799, 2018.
- [16] I. Othman, M. A. Haija, P. Kannan, *et al.*, "Adsorptive removal of methylene blue from water using high-performance alginate-based beads," *Water, Air, & Soil Pollution*, vol. 231, pp. 1-16, 2020.
- [17] J. Xie, R. Lin, Z. Liang, et al., "Effect of cations on the enhanced adsorption of cationic dye in Fe₃O₄-loaded biochar and mechanism," *Journal of Environmental Chemical Engineering*, vol. 9, 2021, Art. no. 105744.
- [18] G. D. Rosa, N. Gostynska, J. W. Ephraim, *et al.*, "Magnesium vs. sodium alginate as precursors of calcium alginate: Mechanical differences and advantages in the development of functional neuronal networks," *Carbohydrate Polymers*, vol. 342, 2024, Art. no. 122375.
- [19] Y. Hu, T. Guo, X. Ye, et al., "Dye adsorption by resins: Effect of ionic strength on hydrophobic and electrostatic interactions," *Chemical Engineering Journal*, vol. 228, pp. 392-397, 2013.
- [20] G. A. El Naeem, A. Abd-Elhamid, O.O. Farahat, et al., "Adsorption of crystal violet and methylene blue dyes using a cellulose-based adsorbent from sugarcane bagasse: characterization, kinetic and isotherm studies," *Journal of Materials Research and Technology*, vol. 19, pp. 3241-3254, 2022.